

## Evidence for exciton fusion as the origin of charge production in molecularly doped polymers

T. E. Orlowski and H. Scher

*Xerox Webster Research Center, Rochester, New York 14644*

(Received 20 December 1982)

Picosecond-pulse- (ultraviolet-) excited photoconductivity measurements in a molecularly doped polymer have provided direct evidence that the dominant mode of charge production in this random molecular system is (triplet-) exciton fusion. The effective rate constant  $\gamma_{\text{eff}}$  of the fusion process is shown to be strongly dependent on the electric field, thus establishing a contribution to the field dependence of the photogeneration yield that cannot be associated with the familiar Onsager process. Time-resolved luminescence measurements in both the picosecond and microsecond range in this system confirm that the time dependence of mobile charge production is controlled by the dynamics of the interacting triplet-exciton population.

### INTRODUCTION

Organic molecules doped into inert polymeric matrices are unique systems for studying both the characteristic photoelectronic and energy transport properties of disordered solids. In these systems interactions between localized sites govern dynamic energy- and charge-transfer properties. There is a growing amount of literature on the study of both singlet- and triplet-exciton migration in these disordered solids<sup>1-3</sup> with particular emphasis on the importance of exciton-annihilation processes as energy-redistribution mechanisms.<sup>2</sup> It would be important as well to know whether exciton annihilation is a viable charge-generation mechanism in these disordered solids as it is in molecular crystals.<sup>4-6</sup> Recently, several papers have appeared concerning the carrier photogeneration and transport properties of aromatic amines in polycarbonate matrices.<sup>7-11</sup> Because these systems are stable (i.e., no crystallization or degradation over a period of months), show no evidence of complex formation, and have high dopant solubility (50 wt. %) which allows for studies of the effect of density of localized sites responsible for photogeneration and transport, they have been regarded as prototypes for studying dynamical charge transfer in disordered organic solids in general. In the system triphenylamine-bisphenol-*A*-polycarbonate (TPA-Lexan) hole photocurrents were found<sup>10</sup> with a photogeneration efficiency  $\Phi$ , which is governed by the Onsager theory of geminate recombination.<sup>12</sup> This theory, as applied to photoionization phenomena, assumes that electron-hole pairs, characterized by a *single* thermalization distance<sup>13</sup>  $r_0$  and a yield  $\Phi_0$ , are produced by absorp-

tion of photons and then either recombine or dissociate into free carriers under the combined influence of the Coulomb attraction and the applied electric field. There is some controversy over whether  $r_0$  should be a constant in these disordered materials<sup>14,15</sup> over large applied field ranges and whether  $\Phi_0$  should be *field independent* as this model assumes.<sup>15</sup> Nevertheless, this phenomenological theory has had much success (and therefore wide acceptance) in explaining the field and temperature dependencies of  $\Phi$  in disordered organic solids<sup>10,16,17</sup> and amorphous selenium.<sup>18</sup> Since the Onsager treatment does not directly address the microscopic processes responsible for carrier photogeneration in disordered molecular solids, several questions can be posed. For example, which electronic state of the photoexcited molecule is most likely to be the precursor to the charge-separated state from which free carriers are formed? Is more than one photon necessary to access this state? What role do surface states play in the photogeneration mechanism in highly absorbing systems, and does one find different mechanisms with bulk excitation? What is the role of "special sites"—often invoked to rationalize one-photon ionization of a relaxed excited molecular state? These and other important issues must be addressed before a more complete understanding of the photogeneration process in disordered molecular solids can be achieved.

In this paper we attempt to answer the above questions by combining optical techniques which *directly* probe the dynamics of the molecular electronic states with photoconductivity measurements which in turn probe photogenerated-carrier densities; in the process we come closer to an understand-

ing of the dominant photogeneration mechanism in certain disordered molecular solids. We report new optical and photoconductivity measurements in the system tri(*p*-tolyl)amine— (TTA-) Lexan, which show for the first time that the dominant mechanism of carrier (hole) photogeneration in this disordered system is *triplet*-exciton fusion and that the effective rate constant  $\gamma_{\text{eff}}$  of the fusion process is highly dependent on the electric field. Previous experiments<sup>9</sup> have identified the charge carrier in this system as the TTA cation,  $\text{TTA}^+$ . We construct a kinetic model for the carrier-photogeneration mechanism, relate our photogeneration efficiency to the familiar Onsager efficiency  $\Phi$ , and show the field regime over which the observed photogeneration yield is *not* controlled solely by the Onsager process. We correlate optical lifetime measurements with photoconductivity data and illustrate how charge production is controlled by the dynamics of the interacting triplet-exciton population.

#### EXPERIMENTAL

The samples were solid solutions of tri(*p*-tolyl)amine (TTA) and bisphenol-*A*-polycarbonate (General Electric Lexan 145) prepared with TTA concentrations between 30 and 40 wt. %. The TTA was purified by multiple recrystallization followed by column chromatography and 100 passes through a zone refiner.<sup>19</sup> Commercially available Lexan was reprecipitated before use. Thin films were cast from dichloromethane solution onto quartz substrates coated with  $\text{SnO}_2$  (200  $\Omega/\text{cm}$ ) using a draw-down coating apparatus under very subdued illumination. Exposure to ultraviolet radiation was eliminated. Residual solvent was driven off by drying in vacuum at 40°C for 2 h. Film thicknesses were 8–12

$\mu\text{m}$ , as determined by cross-section optical microscopy. An electrode (6 mm diameter) consisting of 50-Å Cr covered by 150-Å Au was then vacuum evaporated upon the film surface to complete the sandwich cell geometry for the photoconductivity experiments.<sup>20</sup> Sample films were stored in complete darkness in a desiccator until measurements were made. The apparatus used for photoconductivity and time-resolved photoluminescence measurements is shown schematically in Fig. 1. Single pulses of 7-psec duration from a mode-locked Nd:glass laser were amplified and passed through potassium dihydrogen phosphate (KDP) crystals which generate the 531-nm second harmonic (SHG) and 354-nm third harmonic (THG) of the amplified laser fundamental at 1062 nm. Filters (Schott) were used to block the fundamental (KG-3) and second harmonic (UG-11). Photoconductivity measurements were made using the apparatus shown in the inset of Fig. 1. The excitation pulse was passed through two apertures to reduce off-axis contributions to the laser beam. This provided a more reproducible laser spot size at the sample. Pulse energy at 354 nm was monitored using a calibrated beam splitter and Laser Precision Rj-7100 pyroelectric energy detector-meter. The excitation pulse was weakly focused (area  $A=0.08 \text{ cm}^2$ ) upon the sample illuminating through the quartz substrate and  $\text{SnO}_2$  electrode (86% transmission at 354 nm). Batteries maintained the  $\text{SnO}_2$  electrode at a constant positive bias voltage.<sup>21</sup> Only hole transport is seen in TTA-Lexan as observed in previous studies on this and similar systems.<sup>7–11,16–18</sup> Photocurrents were amplified with a low-noise high dynamic range current amplifier (Ithaco Model 1211) and both displayed in real time  $i(t)$  on a Tektronix 564B storage oscillo-

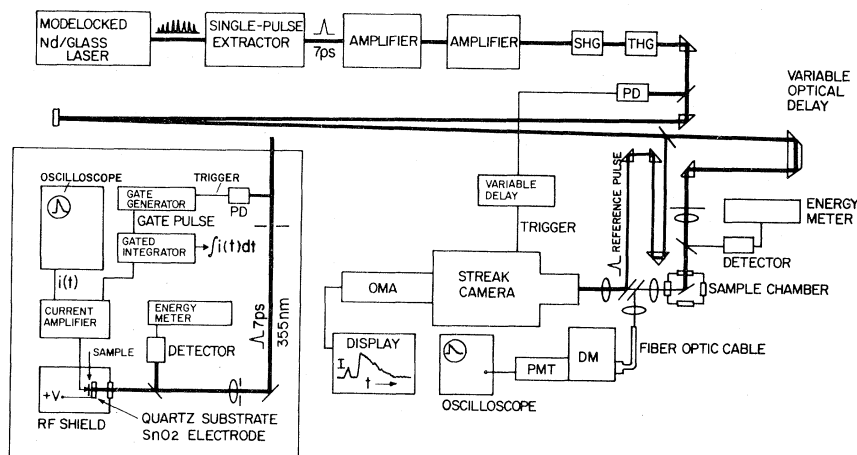


FIG. 1. Schematic diagram of the apparatus used for time-resolved photoluminescence measurements and the photoconductivity apparatus (inset) for determining photogenerated carrier densities.

scope and integrated to obtain the total number of photogenerated carriers,  $q = (1/e) \int i(t) dt$ , with the use of an Evans Model 4130 gated integrator whose output is proportional to the time integral of the input waveform over the duration of a gate pulse. From analysis of the real time data,  $i(t)$ , it was found that, in our samples over the field range studied (5–40 V/ $\mu\text{m}$ ), 200-msec gate pulses were sufficient to collect all the photogenerated charge. These pulses were provided by a gate generator triggered by a photodiode (PD) sampling the excitation pulse. The sample was housed in an rf-shielded enclosure to allow collection of data at very low excitation intensities. Laser pulse energy was varied using calibrated neutral-density filters. All measurements were corrected for dark current. Over the pulse-excitation intensity regime

studied ( $10^{12}$ – $10^{16}$  photons/ $\text{cm}^2$ ), the photoinduced charge was much less than the electrostatic surface charge ( $CV$ ), and thus these measurements are in the small-signal regime. The laser could be fired every 100 sec. Between shots the electrodes were grounded to minimize the accumulation of trapped space charge. Photocurrents measured in this way did not depend on the prior exposure history of the sample.

Time-resolved photoluminescence measurements employed the apparatus shown in the right-hand portion of Fig. 1. This system combines streak camera techniques for resolving fast optical signals (10 psec–10 nsec) with conventional photomultiplier methods for simultaneously measuring slower optical signals (10 nsec–1 sec). The streak camera (Hamamatsu C-979) and optical multichannel analyzer (Princeton Applied Research OMA II) were

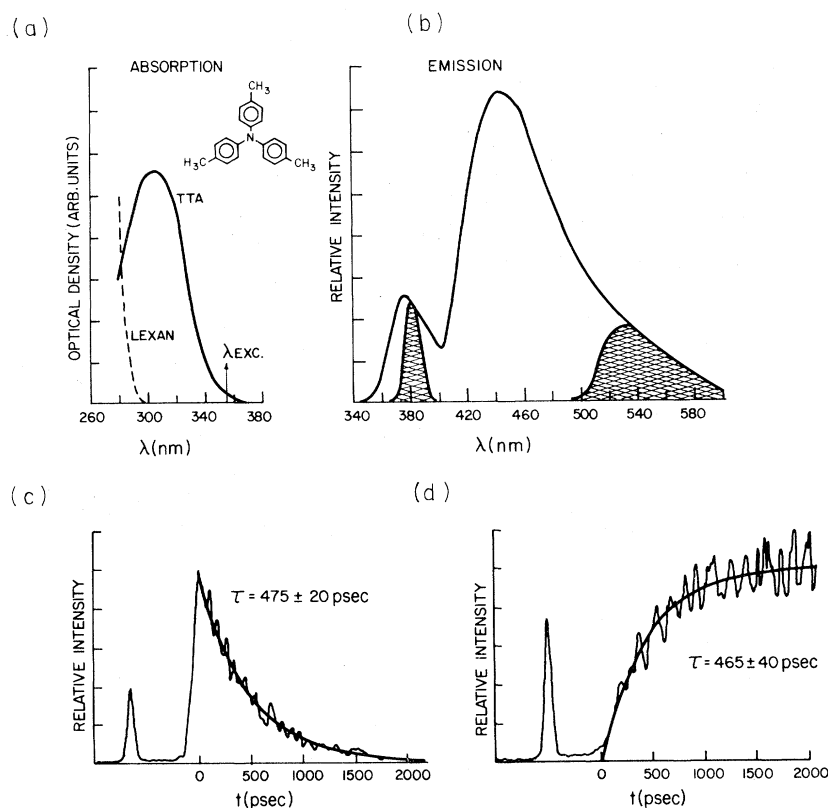


FIG. 2. (a) Absorption spectrum of TTA (solid line) and the onset of absorption in Lexan (dashed line). The arrow depicts the excitation wavelength for all experiments. (b) Emission spectrum of TTA-Lexan (40 wt. %) at room temperature (RT). The peak centered at 375 nm is attributed to TTA fluorescence and the broad band centered at 445 nm is due to TTA phosphorescence. The cross-hatched areas denote the spectral regions isolated for time-resolved measurements of (c) fluorescence decay and (d) phosphorescence buildup, respectively. (c) Fluorescence decay in TTA-Lexan (40 wt. %) at RT obtained using the streak camera shown in Fig. 1. An exponential fit (narrow line) gives a decay time of  $475 \pm 20$  psec. The reference pulse preceding the fluorescence signal illustrates the experimental time resolution and serves as a timing marker for signal averaging purposes. Data from 10 laser shots were averaged. (d) Phosphorescence buildup in TTA-Lexan (40 wt. %) at room temperature. An exponential fit gives a buildup time of  $465 \pm 40$  psec. Data from 25 laser shots were averaged.

used to measure the TTA fluorescence ( $S_1$ ) decay and phosphorescence ( $T$ ) buildup. In these experiments a reference pulse was combined with the sample emission signal with the use of a beam splitter. With appropriate optical delays, the reference pulse preceded the onset of the emission signal facilitating signal averaging of picosecond optical data from successive laser shots. The triplet-exciton lifetime of TTA was measured using a cooled photomultiplier (PMT) and double monochromator (DM) coupled to the experiment with a fiber optic cable.

### RESULTS

Figure 2(a) shows a plot of the absorption spectrum of TTA (solid line) and the onset of absorption in Lexan (dashed line). The arrow at 354 nm indicates the excitation wavelength for our experiments, which lies near the origin of the first singlet transition ( $S_1$ ) of TTA.<sup>22</sup> The absorption coefficient of TTA in Lexan (40 wt. %) is  $\alpha \approx 1700 \text{ cm}^{-1}$  at 354 nm. The absorption depth  $\lambda$ , which will be used to estimate the excitation volume, is  $\alpha^{-1} \sim 6 \mu\text{m}$ . Thus, in this work we have primarily bulk absorption (with  $\sim 10\text{-}\mu\text{m}$ -thick sample) in contrast with the earlier studies<sup>8,10</sup> where excitation at shorter wavelengths produced surface absorption ( $\lambda \sim 0.25 \mu\text{m}$ ). Figure 2(b) shows the emission spectrum of TTA-Lexan (40 wt. %) taken at room temperature using a Perkin-Elmer MPF-44A emission spectrometer with an excitation wavelength of 310 nm. The band centered at 375 nm is attributed to fluorescence from the  $S_1$  state of TTA while the broader band centered at 445 nm is due to phosphorescence from the lowest triplet ( $T$ ) state. These assignments are based upon spectra reported in the literature,<sup>23</sup> time-resolved measurements discussed later, and emission spectra of TTA taken in EPA (ethyl ether:isopentane:ethanol, volume ratio 5:5:2) solution at room temperature and in an EPA glass at 77 K.<sup>24</sup> Previous experiments in solution have shown that the fluorescence quantum yield ( $\Phi_f$ ) in triphenylamine (TPA), a molecule very similar to TTA, is low ( $\Phi_f \approx 0.05$ ), and that intersystem crossing (ISC) is the primary relaxation channel following excitation into  $S_1$ .<sup>25</sup> If we take  $\Phi_f \approx 0.05$  in TTA-Lexan, neglect internal conversion ( $S_1 \rightarrow S_0$ ), and use  $\Phi_{\text{ISC}} \approx 0.95$  (see Ref. 25) then from either the fluorescence decay or phosphorescence buildup times we can obtain a measure of the ISC time. We measured the fluorescence decay time and phosphorescence buildup time in TTA-Lexan using the picosecond laser-streak camera system shown in Fig. 1. The spectral regions isolated for each measurement are shown as cross-hatched areas in Fig. 2(b). The results are displayed in Figs. 2(c) and 2(d).

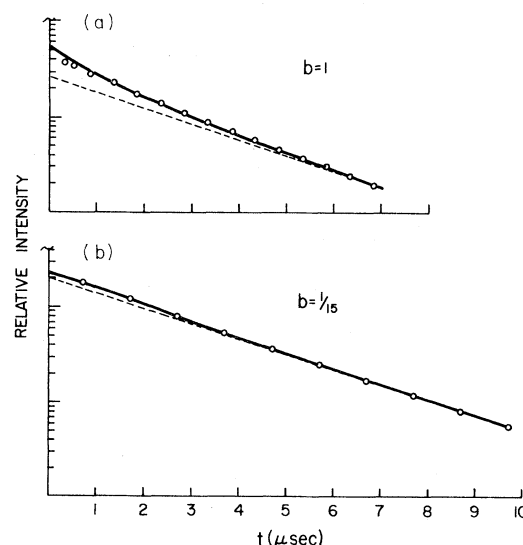


FIG. 3. Phosphorescence decay (520 nm) in TTA-Lexan (40 wt. %) at room temperature and pulse-excitation intensity of  $1.5 \times 10^{15}$  photons/cm<sup>2</sup> in (a) and  $1.0 \times 10^{14}$  photons/cm<sup>2</sup> in (b). The dashed lines with both curves represent the low-intensity triplet-exciton lifetime ( $k^{-1} = 2.70 \pm 0.05 \mu\text{sec}$ ) and the solid lines are fits to Eq. (5) for the triplet-exciton decay with  $b = 1$  in (a) and  $b = 1/15$  in (b). The fits provide a value of  $1.6 \times 10^{-13} \text{ cm}^3/\text{sec}$  for  $\gamma_{\text{eff}}^0$  the effective triplet-exciton fusion rate constant at zero field.

Plotted is the luminescence intensity from  $t = 0$  to 2000 psec. To the left of  $t = 0$  in each figure is a reference pulse which is used as a timing registration marker for signal averaging purposes. It also illustrates the time resolution of these measurements. We find a fluorescence decay time ( $1/e$ ) of  $475 \pm 20$  psec and a phosphorescence buildup time of  $465 \pm 40$  psec. Within experimental error these times are equal ( $470 \pm 30$  psec), and using  $\Phi_{\text{ISC}} \approx 0.95$  we obtain a value of  $495 \pm 30$  psec for the intersystem crossing ( $S_1 \rightarrow T$ ) time of TTA in Lexan. The triplet-exciton lifetime was measured using a photomultiplier and double monochromator as discussed in the experimental section. At 520 nm, we find an initial decay component (representing about 3% of the total decay) which is faster than the time resolution of the PMT ( $\sim 7$  nsec). The remainder of the decay is exponential at low pulse-excitation intensities ( $< 10^{13}$  photons/cm<sup>2</sup>) with a decay time of  $2.70 \pm 0.05 \mu\text{sec}$ . At higher excitation levels the *early-time* behavior is nonexponential (see Fig. 3) and will be discussed later.

Photoconductivity measurements were made on samples containing 40 wt. % TTA in Lexan over a field range of 5–40 V/ $\mu\text{m}$ . Plotted in Fig. 4 is the total number of photogenerated carriers/cm<sup>2</sup>,  $q/A$ , versus pulse-excitation intensity  $I$  (photons/cm<sup>2</sup>) at

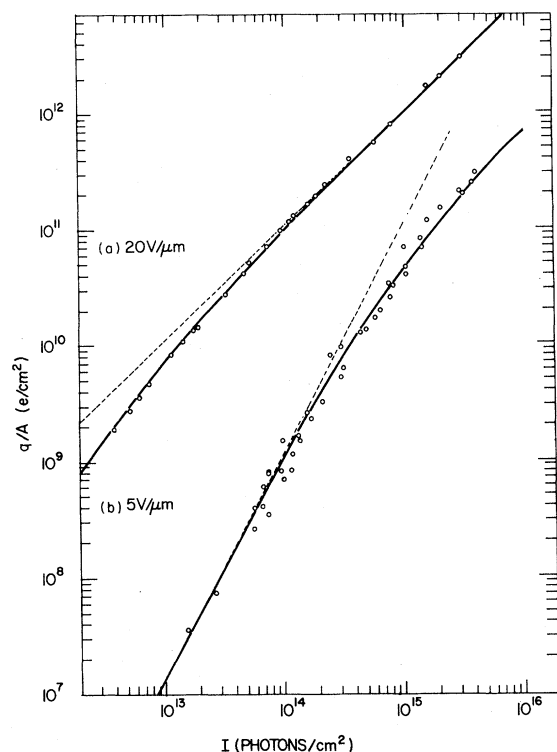


FIG. 4. Total photogenerated carriers/cm<sup>2</sup>,  $q/A$ , in TTA-Lexan (40 wt. %) vs laser-pulse intensity  $I$  at 5 V/ $\mu\text{m}$  and 20 V/ $\mu\text{m}$ . Each data point represents one laser shot. In each case the solid curve is a best fit of Eq. (8) to our data. The dashed lines represent linear and quadratic dependencies of  $q/A$  upon  $I$ . Values of  $\gamma_{\text{eff}}$  and  $\eta_{\text{eff}}$  obtained from these fits and data at other fields are summarized in Table I.

fields of 5 and 20 V/ $\mu\text{m}$ . Each data point represents one laser shot. Also shown are dashed lines representing quadratic and linear dependencies of  $q/A$  upon  $I$ . All measurements were made at room temperature. No change in either the photogeneration efficiency or intensity dependence was found over a period of several months.

Our results may be summarized as follows:

(1) The singlet-exciton lifetime ( $S_1$ ) of TTA in Lexan is  $470 \pm 30$  psec and is governed primarily by intersystem crossing ( $\Phi_{\text{ISC}} \sim 0.95$ ) to the lowest triplet state ( $T$ ) of TTA.

(2) The TTA triplet-exciton decay in Lexan is exponential with a decay time of  $2.70 \pm 0.05$   $\mu\text{sec}$  at low ( $< 10^{13}$  photons/cm<sup>2</sup>) pulse-excitation intensities. The early-time decay becomes nonexponential at higher excitation levels.

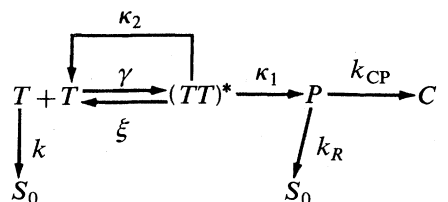
(3) The dependence of the photogeneration yield  $q/A$  upon pulse-excitation intensity  $I$  varies smoothly from  $I^2$  at low intensities to  $I$  at high intensities. This intensity dependence is itself electric field dependent.

## DISCUSSION

### A. Kinetic model: Photogeneration mechanism

Our optical results combined with triplet quantum yield estimates<sup>25</sup> indicate that TTA triplets are formed with high yield within 500 psec in TTA-Lexan following excitation into the  $S_1$  state. These triplets will decay by unimolecular processes (both radiative and nonradiative) and undergo fusion processes<sup>26</sup> due to the small molecular separations at these high concentrations.

We shall present a kinetic model which incorporates just the features *needed* to explain our optical and electrical measurements, which are carried out under identical conditions. The model describes the photogeneration mechanism in this disordered solid involving the TTA triplet-exciton dynamics under conditions of very short pulse excitation (the pulse width is much shorter than the intersystem crossing time). One of the channels of triplet-exciton fusion results in the production of a charge-separated state ( $P$ ) involving some acceptor or acceptor state in the polymer. There are a number of ways that triplet-exciton fusion can generate  $P$ . In some cases, it is assumed that with every encounter one exciton promotes ionization of the other by direct energy transfer and irreversibly returns to the ground state (e.g., generation by singlet-exciton fusion processes in anthracene<sup>4,5</sup>). We will show that this cannot be the dominant process in our case. We instead consider the triplet-exciton fusion process described by Jortner *et al.*<sup>27</sup> and Swenberg<sup>28</sup> and later justified [for three-dimensional (3D) systems] by Suna.<sup>29</sup> The isolated triplets collide and interact to form an associated triplet pair state  $[(TT)^* \equiv T^*]$ , which only in 3D is it meaningful to describe as a nearest-neighbor pair.<sup>29</sup> The model for generation we use is that  $P$  directly results from the closely associated exciton pair i.e., a possible intermediate charge-transfer (CT) state is part of the  $T^*$  state. A schematic diagram of the model is shown below:



Here,  $S_0$  refers to the ground electronic state and  $C$  represents the TTA cation.

The equations describing this scheme are

$$\frac{dT}{dt} = -\gamma T^2 - kT + 2\xi T^* + \kappa_2 T^* \quad (1)$$

$$\frac{dT^*}{dt} = \frac{1}{2}\gamma T^2 - (\xi + \kappa_1 + \kappa_2)T^*, \quad (2)$$

$$\frac{dP}{dt} = \kappa_1 T^* - (k_{CP} + k_R)P, \quad (3)$$

$$\frac{dC}{dt} = k_{CP}P. \quad (4)$$

The form of the kinetic equations is justified under the conditions of this experiment. Namely, the excitation pulse terminates before the population of triplet states (i.e., no possibility for triplet-triplet absorption), and the operative time range is greater than the intersystem crossing time. The supply to the triplet state is incorporated into the initial population  $T_0$ , i.e.,  $\lambda T_0 = \Phi_{ISC}I$ . We also assume there is no nongeminate recombination, i.e., no loss term in Eq. (4) for the cations. The coupling constant  $\gamma$  ( $\xi$ ) describes the diffusion limitation towards (away from) the triplet-exciton fusion process (the energy migration),  $\kappa_1$  describes the part of the annihilation rate of the nearby pair resulting in a charge-separated state, and  $\kappa_2$  describes the annihilation rate resulting in a regenerated  $T$  and a ground-state molecule  $S_0$  (one could also add a process yielding two  $S_0$ , but for our purpose this would only result in a small modification of  $\kappa_2$ ).

The rate constants of the Onsager process are the generation of cations ( $k_{CP}$ ) or recombination ( $k_R$ ) of the separated charge pair. It is well known that these rate constants can be highly  $E$  dependent. The field dependence can be rationalized by the usual model for the Onsager process—diffusion-limited reaction in a continuum in the presence of both the Coulomb and external fields,<sup>12</sup> with a scale parameter  $\Phi_0$  and an initial pair separation parameter  $r_0$ . The novel feature of the present generation process is the strong  $E$  dependence of  $\kappa_1$ . This gives rise to an additional field dependence of the quantum yield  $\Phi$  of cations that is not included in the description of  $\Phi$  in terms of the Onsager model with a field independent  $\Phi_0$ . Nor is this field dependence of  $\kappa_1$  simply a model for  $\Phi_0$ —as will be discussed below.

One can obtain an analytic solution of the system of coupled equations (1)–(4) under the general condition that the lifetime of the  $T^*$  state is short, compared to the triplet-exciton lifetime with an arbitrary lifetime for  $P$ . The triplet-exciton lifetime  $k^{-1}$  is 2.7  $\mu\text{sec}$ , and thus it is quite reasonable to assume  $\xi, \kappa_{1,2} \gg k$ .

The solution for the two physical observables is

$$T(t) = T_0 e^{-kt} [1 + b(1 - e^{-kt})]^{-1}, \quad (5)$$

$$C(t) = \frac{1}{2} \eta \eta_k \gamma_{\text{eff}} \left[ \int_0^t T^2(t') dt' - e^{-k_P t} \int_0^t T^2(t') e^{k_P t'} dt' \right], \quad (6)$$

where

$$\gamma_{\text{eff}} \equiv \gamma (\kappa_1 + \frac{1}{2} \kappa_2) / (\xi + \kappa_1 + \kappa_2), \quad (7)$$

$\eta_k \equiv \kappa_1 / (\kappa_1 + \frac{1}{2} \kappa_2)$ ,  $\eta \equiv k_{CP} / k_P$ ,  $k_P \equiv k_{CP} + k_R$ , and  $b \equiv \gamma_{\text{eff}} T_0 / k$ . It is easy to show (using the Laplace approximation<sup>30</sup>) that the second term in the large parentheses in Eq. (6) can be neglected compared to the first term if  $k_P t, kt \gg 1$ , independent of the magnitude of  $k_P$  relative to  $k$ . We denote  $C(t)$  in this later range as  $C_\infty$  and obtain

$$C_\infty = \frac{1}{2} \eta \eta_k T_0 [1 - b^{-1} \ln(1 + b)]. \quad (8)$$

Equations (5) and (8) will be the basis of the comparison of this kinetic scheme with our measurements. In Fig. 5 we show a plot of  $C_\infty b / (\eta \eta_k T_0)$  as a function of the key parameter  $b$ . In the limit of small  $b$ , where unimolecular decay dominates,  $C_\infty \rightarrow \eta \eta_k \gamma_{\text{eff}} T_0^2 / 4k$  and for large  $b$ , where the decay is essentially bimolecular,  $C_\infty \rightarrow \frac{1}{2} \eta \eta_k T_0$ . An important feature of the  $b$  dependence to note in Fig. 5 is the gradual transition from the quadratic to linear behavior. The transition occurs over a 2–3 decade

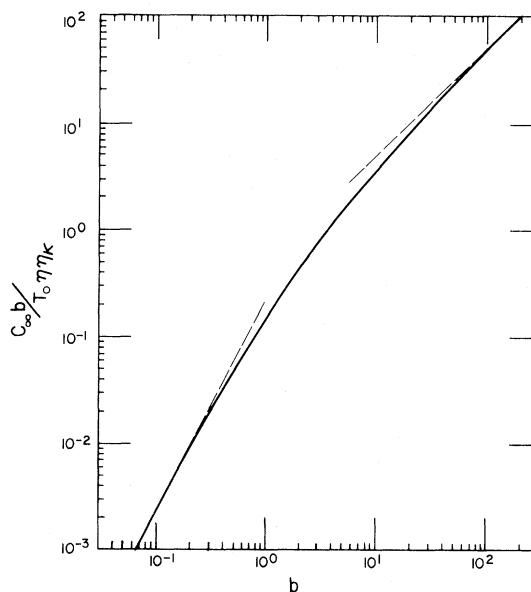


FIG. 5. Theoretical predictions of the kinetic model for photogeneration in TTA-Lexan. The model predicts [see Eq. (8)] a transition in the dependence of  $C_\infty b / \eta \eta_k T_0$  upon  $b$  from quadratic behavior at small  $b$  to linear behavior for large  $b$ . The dashed lines depict the limiting behavior.

TABLE I.  $\gamma_{\text{eff}}$  and  $\eta_{\text{eff}}$  obtained by fitting Eq. (8) to  $q/A$ -vs- $I$  data at the fields shown.  $\gamma_{\text{eff}}$  at  $E=0$  was obtained from a fit of Eq. (5) to the triplet-exciton decay (see Fig. 3).  $\gamma_{\text{eff}}$  at  $E=38 \text{ V}/\mu\text{m}$  could not be determined since  $q/A$  vs  $I$  was linear throughout the range of accessible  $I$  values (see text).

$E$ ( $10^4 \text{ V/cm}$ )	$\gamma_{\text{eff}}$ ( $10^{-12} \text{ cm}^3/\text{sec}$ )	$\eta_{\text{eff}}$ $10^{-4}$
0	$0.16 \pm 0.02$	
5.0	$0.65 \pm 0.15$	$1.0 \pm 0.1$
6.6	$4.8 \pm 1.0$	$1.8 \pm 0.3$
8.3	$14 \pm 6$	$2.0 \pm 0.2$
20.0	$160 \pm 70$	$9.5 \pm 1.5$
38.0		$24 \pm 1$

change in  $b$ . The logarithmic "softness" of this transition as well as the two limiting slopes will play an important role in the analysis of the data.

We assume that the cations are created uniformly throughout the excitation volume  $\lambda A$  in a time that is short compared with the transit time and that they are all collected without deep trapping or nongeminate recombination; thus  $\lambda C_{\infty} = q/A$ . It might be argued that the bulk absorption would increase the chance for nongeminate recombination, as it takes the cation a longer time to transit the excitation volume as compared to the case for strongly absorbed light.<sup>10</sup> However, the concentration of trapped electrons (due to pair ionization) increases in the same proportion as the time to leave the excitation volume decreases. Hence for the same value of  $I$  no advantage is gained by using smaller absorption depths.

### B. Data analysis

In Fig. 4 we show  $q/A$ -vs- $I$  data at fields of 5 and 20  $\text{V}/\mu\text{m}$ . The change in field not only produces a large shift in  $q/A$  (at a fixed  $I$ ) indicative of an  $E$ -dependent  $\Phi$ , but also causes a significant alteration of the intensity dependence. The lower data set clearly shows an  $I^2$  dependence at lower  $I$ , while the upper data set shows an  $I$  dependence at high  $I$ . Thus, there is an  $E$  dependence in both  $q/A$  and in the intensity dependence. In fitting the data to the theoretical curve in Fig. 5 we readily can understand this behavior by admitting an  $E$  dependence of  $b$ . The solid lines in Fig. 4 result from both a vertical and horizontal shift of the curve in Fig. 5. The prime candidate for the field dependence of  $b$  is  $\gamma_{\text{eff}}$ , as  $T_0$  and  $k$  result from intramolecular processes. We determined  $\gamma_{\text{eff}}(E)$  by fitting our  $q/A$ -vs- $I$  data using Eq. (8) at each field with  $\gamma_{\text{eff}}$  the only adjustable parameter. In Table I and the upper portion of Fig. 6, we show the results of this fitting procedure.

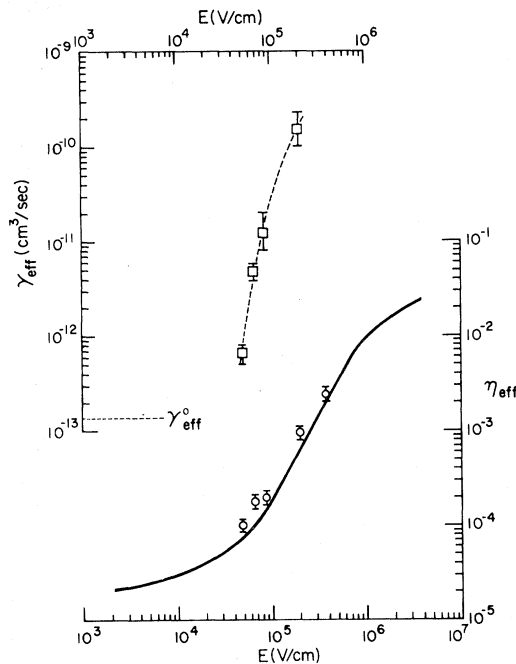


FIG. 6. Shown (upper left) is data (squares) representing the field dependence of  $\gamma_{\text{eff}}$  obtained from a fit of Eq. (8) to our data.  $\gamma_{\text{eff}}^0$  is the triplet-exciton fusion rate constant at zero-field obtained from a fit of Eq. (5) to the triplet-exciton decay (see Fig. 3). Shown (lower right) is data (circles) representing the field dependence of  $\eta_{\text{eff}}$ . Also displayed (solid line) is a fit to the Onsager theory of the results ( $\Phi$  vs  $E$ ) obtained for TPA-Lexan (40 wt. %) from Fig. 4 of Ref. 10.

The values derived for  $\gamma_{\text{eff}}(E)$  are consistent with the direct determination, at zero field, for  $\gamma_{\text{eff}}$  from the phosphorescence decay. In Fig. 3 we fit the triplet-exciton decay to Eq. (5) (solid lines). At the higher excitation level,  $1.5 \times 10^{15} \text{ photons}/\text{cm}^2$ , the deviation from an exponential decay is well accounted for by  $b=1$ . The lower fit represents the change in  $b$  corresponding to a decrease in  $I$  by a factor of 15. Thus the triplet-exciton decay exhibits an intensity dependence that is described by Eq. (5) with  $\gamma_{\text{eff}} = 1.6 \times 10^{-13} \text{ cm}^3/\text{sec}$  and  $k^{-1} = 2.7 \mu\text{sec}$ .

The quantity  $\eta_{\text{eff}}$  also shown in Table I is defined as

$$\eta_{\text{eff}}(E) \equiv \frac{1}{2} \eta_k(E) \eta(E) \Phi_{\text{ISC}}. \quad (9)$$

It is the slope in the linear portion of  $q/A$  vs  $I$  and plays the role of the quantum yield when comparisons are made with data derived from a linear response to excitation intensity. This comparison is made in the lower portion of Fig. 6—the solid line is the fit to the Onsager theory of the  $\Phi$ -vs- $E$  results of a TPA-Lexan film (40 wt. %) from Fig. 4 of Ref. 10. We note a number of remarkable aspects of the

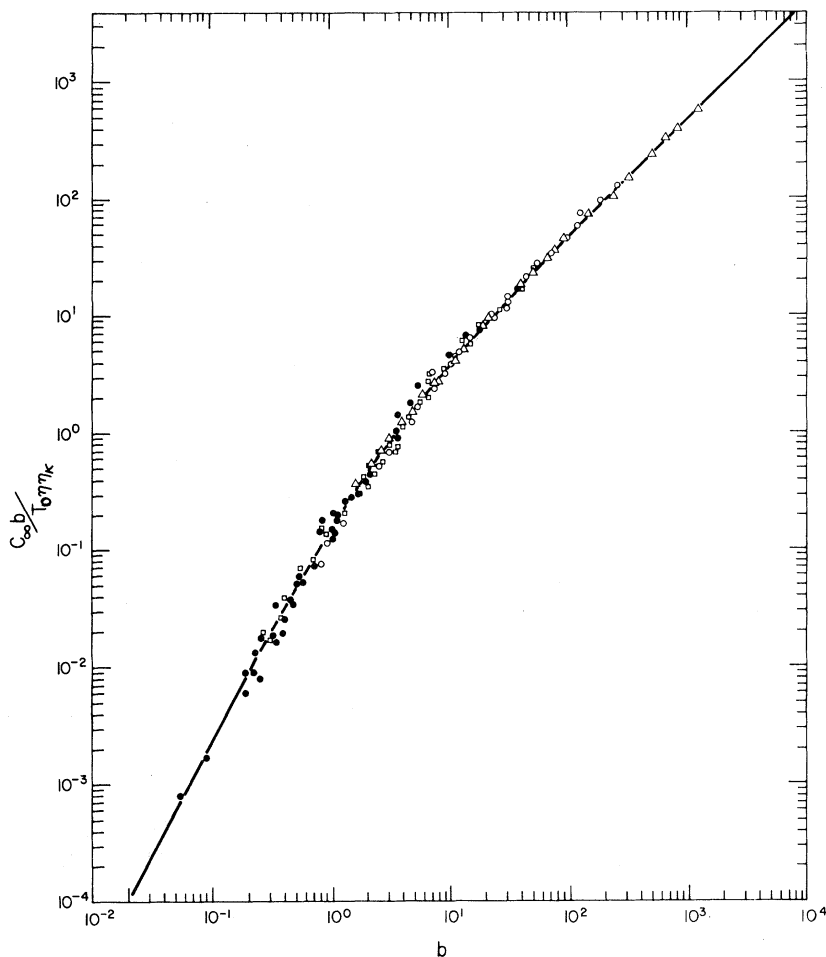


FIG. 7. Composite plot of  $q/A$ -vs- $I$  data in TTA-Lexan (40 wt. %) at fields from 5–20  $V/\mu m$ . The solid line is from Fig. 5. Each data set is plotted using  $\gamma_{\text{eff}}(E)$  values from Table I at the appropriate field to relate  $I$  to  $b$ .

results displayed in Fig. 6: (1) The  $E$  dependence of  $\gamma_{\text{eff}}(E)$  is very strong—a change of  $\sim 2$  orders of magnitude in a narrow field range. (2) The quantum yield  $\eta_{\text{eff}}$  has the same field dependence and very nearly the same magnitude as  $\Phi$  of Fig. 4 in Ref. 10. (The additional value of  $\eta_{\text{eff}}$  at 38  $V/\mu m$  was obtained from  $q/A$ -vs- $I$  data that exhibited a purely linear  $I$  dependence.<sup>31</sup>) (3) A composite (shown in Fig. 7) of the  $q/A$ -vs- $I$  data plotted using  $\gamma_{\text{eff}}(E)$  to relate  $I$  to  $b$  represents an agreement with the curve of Fig. 5 for over six decades of change of  $(q/AI)b/2\eta_{\text{eff}}$ . (4) The zero field  $\gamma_{\text{eff}}$  obtained from optical results is a consistent lower-field limit to the values derived from the photoconductivity measurements.

The zero-field limit and estimate of the saturated value at high field for  $\gamma_{\text{eff}}$  can yield an estimate for  $\eta_k$ . To obtain the field dependence of  $\gamma_{\text{eff}}$  we must have  $\kappa_1/\xi < 1$ . We assume that at zero field  $\kappa_1/\frac{1}{2}\kappa_2 < 1$  (otherwise  $\eta_k \simeq 1$  at all fields). Thus

$\gamma_{\text{eff}}(0) \simeq \frac{1}{2}\gamma\kappa_2/\xi$ . The high-field result yields  $\gamma > 10^{-10}$   $\text{cm}^3/\text{sec}$ . Hence  $\xi/\frac{1}{2}\kappa_2 > 7 \times 10^2$ . Also  $\gamma_{\text{eff}}(E) \simeq (\frac{1}{2}\gamma\kappa_2/\xi)(1 + \kappa_1/\frac{1}{2}\kappa_2)$ , and at 5  $V/\mu m$  one obtains  $\kappa_1/\kappa_2 \sim 2$ , thus  $\eta_k \sim 0.8$  at the low-field value. We can consider  $\eta_k$  slowly varying with  $E$  over our experimental range. However,  $\eta_k$  can vary rapidly with  $E$  at lower fields. The  $E$  dependence of  $\eta_{\text{eff}}(E)$  over our experimental range therefore derives mainly from the Onsager  $\eta(E)$ . This is an important deduction relating to the statement above concerning the minimum generality of the model. If we did not have a  $P$  state, then

$$T^* \xrightarrow{\kappa_1} C, \quad \eta = 1$$

and we could not explain the field dependence of both  $\gamma_{\text{eff}}(E)$  and  $\eta_{\text{eff}}(E)$ . Establishing the necessity of the  $P$  state is one step towards the explanation of the mutual consistency between  $\eta_{\text{eff}}(E)$  and the result of Borsenberger *et al.*<sup>10</sup> This compatibility em-



phasizes that the photogeneration mechanism is most probably the same for TTA-Lexan and the TPA-Lexan system, even though the measurement of the yield was carried out under different conditions—cw illumination versus very short pulse, strongly absorbed light versus bulk absorption, xerographic techniques versus electroded transient current.

There is disagreement, however, with the parameters used by Borsenberger *et al.*<sup>10</sup> to fit their results to the Onsager theory. For sufficiently high  $E$  and/or  $I$  such that  $q/A \propto I$  the value we would obtain for  $\Phi_0$  is  $\Phi_0 = \frac{1}{2} \Phi_{\text{ISC}}$ . While this value is nearly equal to that obtained in Refs. 16 and 17 for photogeneration in other disordered organic solids it is about 1 order of magnitude higher than the one used by Borsenberger *et al.*<sup>10</sup> of  $\Phi_0 \sim 0.03$ . For the range of  $r_0$  needed to obtain a steep  $E$  dependence of  $\eta$ , a small relative decrease in  $r_0$  can easily cause an order-of-magnitude lowering of  $\eta(0)$ . This can be compensated in the fit by a corresponding increase in the high-field saturation value of  $\eta(E)$ . Perhaps more of a concern is the intensity dependence. Borsenberger *et al.*<sup>10</sup> state that they observe a linear (cw) intensity dependence of the discharge rate. The intensity range of their measurements is low:  $10^{12} - 10^{13}$  photons/cm<sup>2</sup> sec. If we can assume that the test for linearity was conducted at high fields and high concentrations we can suggest that the steady-state triplet annihilation rate and the unimolecular decay rate are comparable to within an order of magnitude. This is a sufficient condition to avoid the quadratic dependence in the rate of cation production. The criterion derived from a steady-state solution of Eq. (1) is  $(\gamma_{\text{eff}} I_{\text{cw}} / \lambda)^{1/2} \sim k$ . We find an order-of-magnitude comparison for  $\gamma_{\text{eff}} \sim 10^{-9} - 10^{-10}$  cm<sup>3</sup>/sec,  $I_{\text{cw}} \sim 10^{13}$  photons/cm<sup>2</sup> sec,  $\lambda \sim 0.2$   $\mu\text{m}$ , and  $k \sim 10^5$  sec<sup>-1</sup>. Thus it is entirely possible that the photogeneration mechanism is the same in these similar molecular systems under very different experimental conditions.

As possible alternatives to the explanation of the  $I^2$  dependence one might consider two-photon ionization of TTA or singlet-singlet exciton fusion. Even though the rate of delivery of the photons is very high, the spatial density of photons/pulse is low. For  $I = 10^{13}$  photons/cm<sup>2</sup>, the density of excited TTA molecules is  $1.7 \times 10^{16}$  cm<sup>-3</sup>, which is less than  $10^{-4}$  of the concentration of TTA. Thus the maximum possible yield due to two-photon absorption is  $\sim 10^{-4}$ . At 38 V/ $\mu\text{m}$  we observe a yield of  $2.4 \times 10^{-3}$  for  $I < 10^{13}$  photons/cm<sup>2</sup>. In addition, for a two-photon mechanism the  $I^2$  dependence is usually dominant at the highest pulse intensities; we observe the opposite behavior. The  $S_1$  lifetime is primarily nonradiative and determined mostly by

the intersystem crossing time. There is no  $I$  dependence of the initial decay of  $S_1$  in the regime we did the photoconductivity measurements. This rules out singlet-singlet fusion processes as well as any exciton complex formation (in the time frame of  $\sim 100$  psec).

### C. Processes competing with carrier formation

The consideration of  $\eta_{\text{eff}}$  is not the whole story. In tracking the course of the optical excitation, initially of the TTA  $S_1$  state, one can identify five dissipative processes competing with cation production: (1) the fluorescence of the  $S_1$  state, (2) the use of two triplets to produce one pair state  $P$ , (3) the triplet annihilation leading to products other than  $P$  (4) the recombination of  $P$ , and (5) the unimolecular triplet-exciton decay. Each of the first four is associated with the deviation from unity of one of the four factors of  $\eta_{\text{eff}}$  in Eq. (9). The dissipation due to the unimolecular decay of the triplets shows up as the nonlinear dependence of the quantum efficiency  $\Phi \equiv q/AI$  on  $I$ . Strictly,  $\Phi = \eta_{\text{eff}}$  only in the linear region. The field  $E$  exerts a strong influence on  $\gamma_{\text{eff}}$  in the field range used in the present measurement (for the 40% film). The value of  $\gamma_{\text{eff}}$  determines the outcome of the competition between triplet annihilation (with the possibility of ion-pair production) and the pure dissipation of the nonradiative decay with rate constant  $k$ . Thus, the  $E$  field can control the effectiveness of the loss due to unimolecular decay. This in turn has a strong effect on the value of  $\Phi$  and hence contributes an important  $E$  dependence to  $\Phi$  that cannot be associated with the Onsager process (or even to a modification, e.g., a field dependent  $\Phi_0$ ). This is convincingly seen in Fig. 4. At  $I = 10^{13}$  photons/cm<sup>2</sup> a change in  $E$  by a factor of 4 causes a 3-decade change in the value of  $\Phi$ . At  $I = 10^{14}$  photons/cm<sup>2</sup> the same change in  $E$  causes a 2-decade increase in  $\Phi$  and only at  $I = 10^{15}$  photons/cm<sup>2</sup> does the 1-decade change in  $\Phi$  reflect the 1-decade change in  $\eta_{\text{eff}}$  (see Table I). (Also note that at  $10^{15}$  photons/cm<sup>2</sup> the 5-V/ $\mu\text{m}$  data set starts to deviate from  $I^2$  behavior.) Thus in this kinetic scheme  $\gamma_{\text{eff}}(E)$  has a significant effect on the value of  $\Phi$  although it does not appear explicitly in  $\eta_{\text{eff}}(E)$ . We can summarize the effect of the electric field as tilting the competition between annihilation of colliding triplets or migration apart, between the production of a separated pair state or another product of annihilation, and between the ionization or recombination of the pair state.

It was important to observe clearly the  $I^2$  dependence of  $q/A$  for the 40% sample to establish the validity of the triplet-exciton fusion photogeneration pathway. Except for the lower  $I$  range of the low-field (5-V/ $\mu\text{m}$ ) data, most of the  $q/A$  data exhibits

at least a quasilinear  $I$  dependence. The observation of the  $I^2$  dependence puts great demands on this system. At  $I = 10^{13}$  photons/cm<sup>2</sup>,  $\Phi \sim 10^{-6}$ . This is 1 order of magnitude lower than the smallest value of  $\Phi$  measured in Ref. 10. In the range of low quantum yields one would expect a number of possibilities to compete with the exciton fusion mechanism, e.g., one-photon ionization at the surface or "special sites." No deviation of  $q/A$  from  $I^2$  behavior at low  $I$  is a strong indication that the unimolecular triplet-exciton decay or an autoionization of  $S_1$  is not associated with cation yields. The fact that another mechanism does not obscure this low  $\Phi$  region is a unique feature of the molecularly doped polymer system.

#### D. Effect of dopant concentration

In Fig. 8, we show the clear  $I^2$  dependence of  $q/A$  for a 30% TTA concentration film. We also show the fit at the highest field (40 V/ $\mu$ m) to the theory (solid line). The lower-concentration film thus also establishes the  $I^2$  dependence, but one cannot definitely demonstrate the transition to the linear  $I$  dependence. The value for  $\gamma_{\text{eff}}$  derived by the fit (at 40 V/ $\mu$ m) is in the range  $10^{-13}$ – $10^{-12}$  cm<sup>3</sup>/sec, the same range as  $\gamma_{\text{eff}}$  at low fields for the 40% sample. We speculate that the  $\kappa_1$  process is strongly  $E$  dependent for the 30% film—however, the effective threshold has been shifted to higher field. Further experiments, including lifetime studies, are planned for the lower concentration films.

We thus conclude that the process giving rise to  $\gamma_{\text{eff}}$  is highly field and concentration dependent. The change in  $\gamma_{\text{eff}}$  is much too large and in the opposite direction to consider the change due to  $E$ -dependent energy migration.<sup>32</sup> Hence  $\xi$  and/or  $\kappa_2$  must be considered. The  $E$  field swings the effective fusion rate of triplets across the entire range of values measured for a series of aromatic crystals—from naphthalene ( $3.5 \times 10^{-12}$  cm<sup>3</sup>sec<sup>-1</sup>) to tetracene ( $2.2 \times 10^{-9}$  cm<sup>3</sup>sec<sup>-1</sup>)—determined from time-resolved delayed fluorescence experiments (cf. Table I.15, p. 139 of Ref. 26). The field also swings  $\gamma_{\text{eff}}$  from annihilation rate limited  $\gamma_{\text{eff}}(0) \sim \frac{1}{2}\kappa_2$  to migration rate limited  $\gamma_{\text{eff}}(E > 20 \text{ V}/\mu\text{m}) < \gamma \sim 10^{-9}$  cm<sup>3</sup>sec<sup>-1</sup>. The fact that the triplet-exciton migration rate can be high in a disordered molecular solid has already been established. Burkhart and Lonson<sup>2</sup> have shown that the diffusion coefficient for triplet energy migration  $D$  is an order of magnitude larger in anthracene-doped polystyrene ( $D \sim 5 \times 10^{-3}$  cm<sup>2</sup>/sec) than in anthracene crystals<sup>33</sup> ( $D \sim 5 \times 10^{-4}$  cm<sup>2</sup>/sec) even though the anthracene intermolecular separations are smaller in the crystal. The large change in  $\gamma_{\text{eff}}(E)$  precludes the fusion process (dis-

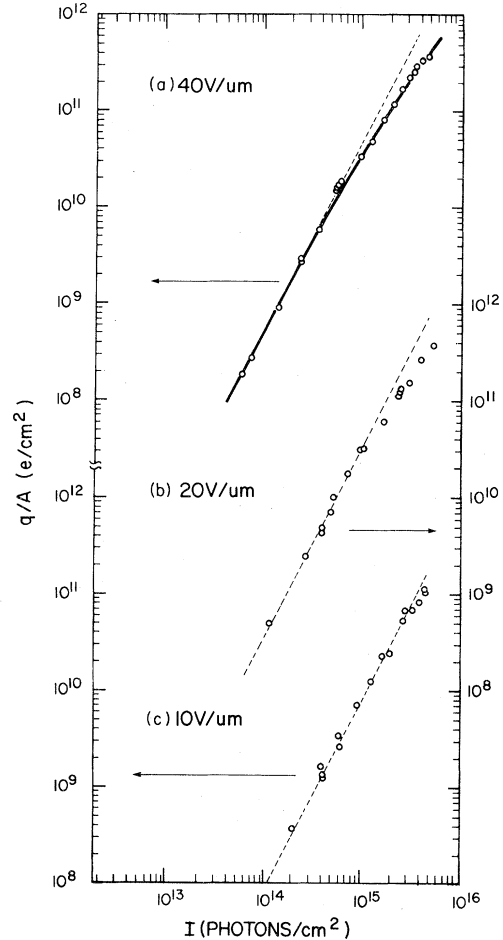


FIG. 8. Total photogenerated carriers/cm<sup>2</sup>,  $q/A$ , in TTA-Lexan (30 wt. %) vs laser-pulse intensity  $I$ , at (a) 40 V/ $\mu$ m, (b) 20 V/ $\mu$ m, and (c) 10 V/ $\mu$ m. In (a) the solid curve is a best fit of Eq. (8) to our data. In (b) and (c) the dashed lines represent a quadratic dependence of  $q/A$  upon  $I$ .

cussed earlier) whereby one exciton returns to the ground state (at each encounter) while the other is excited to a higher state. The largest change in  $\gamma_{\text{eff}}$  with the later process is a factor of 2. This can be seen by first setting  $\xi = 0$  in  $\gamma_{\text{eff}}$ . If we now vary  $\kappa_1$  from  $\kappa_1 < \frac{1}{2}\kappa_2$  to  $\kappa_1 \gg \frac{1}{2}\kappa_2$  we note that  $\gamma_{\text{eff}}$  changes from  $\frac{1}{2}\gamma$  to  $\gamma$ . The inclusion of any other annihilation channel would even further decrease the relative change in  $\gamma_{\text{eff}}$ . Thus we must have  $\xi \gg \kappa_2$  to understand the field dependence of  $\gamma_{\text{eff}}$ .

#### E. Field dependence of $\gamma_{\text{eff}}$

The steepness of the  $E$  dependence of  $\gamma_{\text{eff}}(E)$  in Fig. 6 suggests a field-induced tunnel ionization<sup>34</sup> similar to that observed for the electron ionization rate from deep levels in semiconductors.<sup>35</sup> One can

envison a number of similar possibilities for the ionization of the associated exciton pair  $T^*$ . The electron can tunnel from an excited triplet or singlet state (produced by energy transfer within the associated exciton pair) to an acceptorlike state in the polymer or to an impurity acceptor, e.g., oxygen.<sup>36</sup> Another model based on a small polaron transition between inequivalent sites<sup>37</sup> can account for some of the field dependence. However, to be in the tunneling regime at room temperature requires an intramolecular vibrational mode of energy  $\hbar\omega \sim 100$  meV. For a 10-Å separation between sites the field can affect a 20-meV change in the electronic levels which is only  $\sim 0.2\hbar\omega$  (cf. Fig. 3. in Ref. 37). Jortner *et al.*<sup>27</sup> discuss triplet annihilation with a reaction product of an intermediate ion pair on two neighboring molecules. It is therefore highly suggestive that  $\kappa_1$  itself could be controlled by an Onsager process with  $r_0 \sim 10$  Å. For a dielectric constant  $\sim 3$  the threshold field is  $\sim 1$  V/ $\mu\text{m}$ . At this magnitude of  $r_0$  the field dependence of  $\Phi$  would be very steep (change of 2 orders of magnitude for a change in  $E$  of a factor of 4). However, it is unlikely that a relaxed ion pair could readily recombine to form the two triplets of  $T^*$  as would be required in this kinetic scheme. A plausible picture, combining some of the attributes of the above, should emphasize the admixture of real or virtual states of  $T^*$ . The linear combination of states can include the two triplets, an energy transfer promoting one of the triplets to a higher excited state, and an *excited* charge-transfer complex. The presence of an electric field could promote ionization of the CT state by tunneling to the pair state  $P$ . This picture includes field-induced tunneling and the strong interaction between the associated exciton pair state and the CT complex. The description involving a coupling between a CT pair and an excited exciton state is also in accord with the work of Siebrand and co-workers<sup>38</sup> and the observations of Sebastian *et al.*<sup>39</sup> Further theoretical and experimental work (described in the Summary) will be needed to account for more of the details of the process driving  $\gamma_{\text{eff}}(E)$ .

### SUMMARY

Our findings may be summarized as follows:

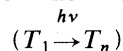
- (1) The combination of sensitive detection of transient photocurrents and time-resolved luminescence (under identical pulse-excitation conditions) has established that the precursor of the dominant mode of charge production in a model disordered molecular solid (TTA-Lexan) is triplet-exciton fusion.
- (2) The effective triplet-exciton fusion rate  $\gamma_{\text{eff}}$  is shown to be highly field dependent—increasing by 2 orders of magnitude for an increase in electric field

of a factor of 4.

(3) The field dependence of  $\gamma_{\text{eff}}$  contributes an important  $E$  dependence to the photogeneration quantum yield  $\Phi$  that is not included in the usual treatment of the Onsager model.

(4) The quantum yield  $\eta_{\text{eff}}$  governing the linear intensity behavior of  $q/A$  in these short-pulse—bulk-excitation experiments is shown to be very similar in magnitude and field dependence to previous measurements (Ref. 10) on the TPA-Lexan system using cw surface excitation and xerographic discharge techniques.

Much is still to be learned in this model disordered solid. Experiments in progress are probing in more detail the concentration and field dependence of  $\gamma_{\text{eff}}$  by measuring the TTA  $S_1$  and  $T$  dynamics optically as a function of these parameters. In addition, photocurrent measurements will be repeated at various temperatures to try and isolate the process responsible for the dramatic field dependence of  $\gamma_{\text{eff}}$ . We also intend to perform experiments utilizing a delayed multiple pulse-excitation scheme where the initial excitation pulse at 354 nm is followed at a later (variable) time by an excitation pulse at 531 nm, near the triplet-triplet absorption maximum<sup>24</sup> of TTA in Lexan. In these experiments, we hope to determine whether excited state absorption processes



also lead to carrier formation.<sup>40</sup> If so, various combinations of excitation pulse intensity and delay time can probe in more detail the dynamics of the overall photogeneration process.

The results of the present study indicate that a new approach to the Onsager process is needed and one is in progress.<sup>41</sup> The intermediate ion pair, e.g., the CT state, and the  $P$  state should be treated on the same footing. The new approach will emphasize a complete (discrete) molecular framework for the Onsager process with the excess charge hopping from site to site in the presence of both Coulomb and uniform field. The initial field-induced tunneling process, based perhaps on the work of Ref. 38, can then be included as a time-dependent source.

### ACKNOWLEDGMENTS

The assistance of Jack Yanus, who purified materials and prepared the films, and of Mike Morgan, who prepared the electrodes for photoconductivity measurements, is gratefully acknowledged. We thank R. W. Anderson for several helpful discussions, a critical reading of the manuscript, and permission to use his unpublished results. The experimental assistance of Charles Woodward and Wayne Knox is also acknowledged.

- <sup>1</sup>G. E. Johnson, *Macromolecules* **13**, 145 (1980); **13**, 839 (1980).
- <sup>2</sup>R. D. Burkhart and E. R. Lonson, *Chem. Phys. Lett.* **54**, 85 (1978); R. D. Burkhart, *Chem. Phys.* **46**, 11 (1980); R. D. Burkhart and A. A. Abla, *J. Phys. Chem.* **86**, 468 (1982); W. Klöpffer, *Chem. Phys.* **57**, 75 (1981).
- <sup>3</sup>C. L. Renschler and L. R. Faulkner, *J. Am. Chem. Soc.* **104**, 3315 (1982); *Faraday Discuss. Chem. Soc.* **70**, 311 (1980).
- <sup>4</sup>M. Pope, H. Kallmann, and J. Giachino, *J. Chem. Phys.* **62**, 2540 (1965).
- <sup>5</sup>C. L. Braun, *Phys. Rev. Lett.* **21**, 215 (1968).
- <sup>6</sup>E. L. Frankevich, M. M. Tribel, I. A. Sokolik, and B. V. Kotov, *Phys. Status Solidi A* **40**, 655 (1977).
- <sup>7</sup>G. Pfister, S. Grammatica, and J. Mort, *Phys. Rev. Lett.* **37**, 1360 (1976).
- <sup>8</sup>G. Pfister, *Phys. Rev. B* **16**, 3676 (1977).
- <sup>9</sup>A. Troup, J. Mort, S. Grammatica, and D. J. Sandman, *J. Non-Cryst. Solids* **35-36**, 151 (1980).
- <sup>10</sup>P. M. Borsenberger, L. E. Contois, and D. C. Hoesterey, *J. Chem. Phys.* **68**, 637 (1978).
- <sup>11</sup>P. M. Borsenberger, W. Mey, and A. Chowdry, *J. Appl. Phys.* **49**, 273 (1978).
- <sup>12</sup>L. Onsager, *Phys. Rev.* **54**, 554 (1938); *J. Chem. Phys.* **2**, 599 (1934).
- <sup>13</sup>R. H. Batt, C. L. Braun, and J. F. Horning, *J. Chem. Phys.* **49**, 1967 (1968).
- <sup>14</sup>M. Yokoyama, Y. Endo, and H. Mikawa, *Bull. Chem. Soc. Jpn.* **49**, 1538 (1976).
- <sup>15</sup>E. A. Silinich, V. A. Kolesnikov, I. J. Muzikante and D. R. Balode, *Phys. Status Solidi B* **113**, 379 (1982).
- <sup>16</sup>G. Pfister and D. J. Williams, *J. Chem. Phys.* **61**, 2416 (1974); P. M. Borsenberger, L. E. Contois, and A. I. Ateya, *J. Appl. Phys.* **50**, 914 (1979).
- <sup>17</sup>P. J. Melz, *J. Chem. Phys.* **57**, 1694 (1972).
- <sup>18</sup>D. M. Pai and R. C. Enck, *Phys. Rev. B* **11**, 5163 (1975).
- <sup>19</sup>Chromatographic techniques revealed an impurity which slowly formed (days). It was removed by sublimation and only freshly sublimated TTA was used to prepare sample films.
- <sup>20</sup>This electrode combination provided high optical transmission at 355 nm and low dark current. Photocurrents with other electrode configurations (SnO<sub>2</sub>-Al, Cr-Au-Cr-Au), when corrected for dark current and optical transmission, were identical to the results reported here.
- <sup>21</sup>Indium contacts were used for both electrodes. Identical results were found, however, with the use of silver paint contacts.
- <sup>22</sup>H. Jaffe and M. Orchin, *Theory and Applications of Ultraviolet Spectroscopy* (Wiley, New York, 1962).
- <sup>23</sup>M. Kasha, H. R. Rawls, and M. Ashrof El-Bayoumi, *Pure Appl. Chem.* **11**, 371 (1965).
- <sup>24</sup>R. W. Anderson (unpublished).
- <sup>25</sup>E. B. Sveshnikova and M. I. Snegov, *Opt. Spectrosc.* **29**, 265 (1970); A. A. Lamola and G. S. Hammond, *J. Chem. Phys.* **43**, 2129 (1965). Sveshnikova and Snegov measure a triplet quantum yield  $\Phi_{ISC}$  of 1.0±0.1 for TPA in benzyl alcohol. Lamola and Hammond measure  $\Phi_{ISC}$ =0.9 for TPA in benzene. We shall use the value  $\Phi_{ISC}$ ≈0.95 as our estimate of the triplet quantum yield of TTA in Lexan.
- <sup>26</sup>For a general review, see M. Pope and C. E. Swenberg, *Electronic Processes in Organic Crystals* (Oxford, New York, 1982).
- <sup>27</sup>J. Jortner, S. I. Choi, J. L. Katz, and S. A. Rice, *Phys. Rev. Lett.* **11**, 323 (1963).
- <sup>28</sup>C. E. Swenberg, *J. Chem. Phys.* **51**, 1753 (1969).
- <sup>29</sup>A. Suna, *Phys. Rev. B* **1**, 1716 (1970).
- <sup>30</sup>E. T. Copson, *Asymptotic Expansions* (Cambridge University Press, Cambridge, England, 1965), Chap. 5.
- <sup>31</sup>There is excellent agreement between  $\eta_{eff}(E)$  and measurement of  $\Phi$  in the TTA-Lexan system using 300-nm excitation and the xerographic discharge technique, J. Mort and S. Grammatica (unpublished).
- <sup>32</sup>J. S. Patel and D. M. Hanson, *J. Chem. Phys.* **75**, 5203 (1981).
- <sup>33</sup>S. Singh, W. J. Jones, W. Siebrand, B. P. Stoicheff, and W. G. Schneider, *J. Chem. Phys.* **42**, 330 (1965).
- <sup>34</sup>S. Makram-Ebeid and M. Lannoo, *Phys. Rev. Lett.* **48**, 1281 (1982).
- <sup>35</sup>D. V. Lang, *J. Appl. Phys.* **45**, 3014 (1974); **47**, 3587 (1976).
- <sup>36</sup>C. L. Greenstock, A. B. Ross, and W. P. Helman, *Radiat. Phys. Chem.* **17**, 247 (1981), and references therein.
- <sup>37</sup>H. Scher and T. Holstein, *Philos. Mag. B* **44**, 343 (1981).
- <sup>38</sup>P. J. Bounds and W. Siebrand, *Chem. Phys. Lett.* **75**, 414 (1980); **85**, 496 (1982); P. J. Bounds, P. Petelenz, and W. Siebrand, *Chem. Phys.* **63**, 303 (1981).
- <sup>39</sup>L. Sebastian, G. Weiser, and H. Bässler, *Chem. Phys.* **61**, 125 (1981); L. Sebastian, G. Weiser, G. Peter, and H. Bässler, *Chem. Phys.* **75**, 103 (1983).
- <sup>40</sup>Biphotonic (sequential) photoionization involving triplet intermediates in disordered organic solids has been reported. See, G. E. Johnson and A. C. Albrecht, *J. Chem. Phys.* **44**, 3179 (1966); K. D. Cadogan and A. C. Albrecht, *ibid.* **51**, 2710 (1969).
- <sup>41</sup>H. Scher and S. Rackovsky (unpublished).